

Reentry Breakup and Survivability Characteristics of the Vehicle Atmospheric Survivability Project (VASP) Vehicles

5 August 2008

Richard G. Stern
Imagery Programs Division
National Systems Group

Prepared for

Space and Missile Systems Center
Air Force Space Command
483 N. Aviation Blvd.
El Segundo, CA 90245-2808

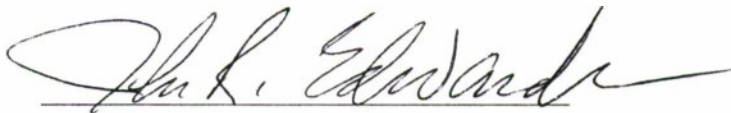
Authorized by: Systems Planning & Engineering

20081230011

This report was submitted by The Aerospace Corporation, El Segundo, CA 90245-4691, under Contract No. FA8802-04-C-0001 with the Space and Missile Systems Center, 483 N. Aviation Blvd., El Segundo, CA 90245. It was reviewed and approved for The Aerospace Corporation by Valerie I. Lang, Principal Director, Office of Chief Architect/Engineer. Mr. John R. Edwards and Mr. Vincent R. Caponpon were the project officers for this study.

This report has been reviewed by the Public Affairs Office (PAS) and is releasable to the National Technical Information Service (NTIS). At NTIS, it will be available to the general public, including foreign nationals.

This technical report has been reviewed and is approved for publication. Publication of this report does not constitute Air Force approval of the report's findings or conclusions. It is published only for the exchange and stimulation of ideas.

A handwritten signature in dark ink, appearing to read "John R. Edwards", with a long, sweeping horizontal stroke extending to the right.

John R. Edwards
SMC/EA

REPORT DOCUMENTATION PAGE			Form Approved OMB No. 0704-0188	
<small>Public reporting burden for this collection of information is estimated to average 1 hour per response, including the time for reviewing instructions, searching existing data sources, gathering and maintaining the data needed, and completing and reviewing this collection of information. Send comments regarding this burden estimate or any other aspect of this collection of information, including suggestions for reducing this burden to Department of Defense, Washington Headquarters Services, Directorate for Information Operations and Reports (0704-0188), 1215 Jefferson Davis Highway, Suite 1204, Arlington, VA 22202-4302. Respondents should be aware that notwithstanding any other provision of law, no person shall be subject to any penalty for failing to comply with a collection of information if it does not display a currently valid OMB control number. PLEASE DO NOT RETURN YOUR FORM TO THE ABOVE ADDRESS.</small>				
1. REPORT DATE (DD-MM-YYYY) 05-08-2008		2. REPORT TYPE		3. DATES COVERED (From - To)
4. TITLE AND SUBTITLE Reentry Breakup and Survivability Characteristics of the Vehicle Atmospheric Survivability Project (VASP) Vehicles		5a. CONTRACT NUMBER FA8802-04-C-0001		
		5b. GRANT NUMBER		
		5c. PROGRAM ELEMENT NUMBER		
6. AUTHOR(S) Richard G. Stern		5d. PROJECT NUMBER		
		5e. TASK NUMBER		
		5f. WORK UNIT NUMBER		
7. PERFORMING ORGANIZATION NAME(S) AND ADDRESS(ES) The Aerospace Corporation Physical Sciences Laboratories El Segundo, CA 90245-4691		8. PERFORMING ORGANIZATION REPORT NUMBER TR-2008(8506)-3		
9. SPONSORING / MONITORING AGENCY NAME(S) AND ADDRESS(ES) Space and Missile Systems Center Air Force Space Command 483 N. Aviation Blvd. El Segundo, CA 90245		10. SPONSOR/MONITOR'S ACRONYM(S) SMC		
		11. SPONSOR/MONITOR'S REPORT NUMBER(S)		
12. DISTRIBUTION/AVAILABILITY STATEMENT Approved for public release; distribution unlimited.				
13. SUPPLEMENTARY NOTES				
14. ABSTRACT The breakup of two satellites (Vehicle Atmospheric Survivability Project) during atmospheric reentry is documented. The satellites were deboosted from orbit, and their subsequent reentries were observed by surface-based radars and optics as well as airborne optics. Numerous pieces of satellite debris were tracked, and, in some cases, their heritage identified. The breakup process substantiated the heating relationships derived from the VAST test, which is an order of magnitude less than traditional heating relationships above an altitude of 30 nmi.				
15. SUBJECT TERMS Satellite reentry breakup, Satellite debris, Aerothermal heating				
16. SECURITY CLASSIFICATION OF:			17. LIMITATION OF ABSTRACT	18. NUMBER OF PAGES 21
a. REPORT UNCLASSIFIED	b. ABSTRACT UNCLASSIFIED	c. THIS PAGE UNCLASSIFIED		
				19b. TELEPHONE NUMBER (include area code) (310)336-4278

Preface

The author of this report was The Aerospace Corporation lead for the VAST and VASP tests conducted from 1971 through 1973. The preflight objectives of the tests were established by The Aerospace Corporation. Post-flight tasks were also defined by The Aerospace Corporation for the various supporting contractors. This report summarizes some of the test results obtained over 35 years ago. The importance of the results is significant because of the assets then available for such tests.

The information contained in this report is condensed from working papers generated by The Aerospace Corporation and contractors supporting the tests. Belated thanks are offered to those contractors (circa 1973), including RCA, AVCO Research, and Lockheed Space and Missile Systems.

Contents

1.	Introduction	1
2.	History	3
3.	VAST and VASP Experiments.....	5
3.1	The Vehicle Atmospheric Survivability Project (VASP)	6
4.	Vehicle Description	9
5.	VASP Breakup Sequence.....	11
6.	Debris Impact Area.....	15
7.	Hardware Impacting Around Eniwetok	19
8.	Summary and Conclusions.....	21
	References	23

Figures

1.	In-board profile VASP vehicle.	9
2.	VASP 1 spread of fragments in X-Y plane from debris mapping.	15
3.	VASP 1 predicted spread of fragments in X-Y plane at impact.	16
4.	Projected impact points of selected tracked objects of VASP 2 reentry.	18

Tables

1. Principal Resources	5
2. Support Summary	6
3. Estimated Aerodynamic Characteristics of Various Subsystems	10
4. Significant Events Test 9265 (SV-5).....	11
5. Significant Events Test 6337 (SV-6).....	12
6. Probable Components Projected to Impact In or Near Eniwetok Lagoon	19
7. VAST Empirical Heating Rates.....	22

1. Introduction

The breakup characteristics of a satellite during atmospheric reentry are documented. Aluminum, magnesium, steel, titanium, glass, beryllium, and copper objects were tracked. The objects ranged in radar cross sections from 1 in² to 10 ft². Several clouds of copper droplets in the form of dipoles were detected, which provided apparent radar cross sections an order of magnitude greater than the satellite from which they emerged. The extent of the impact pattern and its makeup is also described. Low-ballistic-coefficient objects were surprisingly observed throughout the debris footprint.

The purpose of this report is to provide wider exposure of the results, which has been limited to a few Air Force programs. The information is based upon working papers and data accumulated in 1973.

The Vehicle Atmospheric Survivability Project (VASP) was conducted during the closing years of the Safeguard Program. The goal of the Safeguard program was to develop an anti-ballistic missile system that could discriminate warheads from decoys and booster rocket debris produced during reentry. The numerous assets supporting Safeguard were available and appropriate for VASP. The availability to VASP of personnel and equipment was enhanced by presidential priority given to the VASP effort. The Safeguard program was disbanded after the anti-ballistic missile treaty with the Soviet Union of the early 1970s (entered into force 3 October 1972). The assets and personnel supporting Safeguard were significantly reduced. A project such as VASP would be near impossible without the assets and the presidential priorities then available. It is noted that fewer tracking assets and analysts were available for the VASP tests (conducted post treaty in 1973) than were available for the VAST tests (conducted prior to October 1972). The quantity and quality of data collected on VASP was less than that for VAST, which was conducted prior to the antiballistic missile treaty.

The test results demonstrate that traditional aerodynamic heating estimates are in error by an order of magnitude above an altitude of 30 nmi. The tests also indicate that, in some cases, traditional aerodynamic heating results may not always apply below an altitude of 30 nmi.

2. History

Six satellite reentry tests were conducted over three decades ago (1971–1973). These tests were authorized by the Office of the Secretary of the Air Force (OSAF) at the request of White House staff members. The objective of the tests was limited to experimentally determining the reentry survivability and condition of vehicle payload elements. A by-product of the tests was an insight into a satellite's aerothermal breakup process.

The breakup phenomenon observed revealed that, contrary to theory, breakup was essentially independent of attitude behavior and geometry. In addition, the heating encountered by the reentering satellite was an order of magnitude less than theory would indicate. These revelations were utilized in deboost and strategy policy for those Air Force Low Earth Orbiting (LEO) satellite vehicles directly under the OSAF.

For several decades, knowledge of the reentry tests remained limited to personnel involved with the OSAF's LEO programs. Academia, most satellite and launch vehicle contractors, and other government agencies remained unaware of the experiments.

In 1983 (a decade after the last reentry test), an OSAF Air Force satellite program was scheduled to be launched from Vandenberg AFB by the Space Shuttle. The satellite's mission profile and design required that it be launched into an elliptical orbit with almost a 400 nmi apogee altitude. NASA analysis indicated that the mission could not be safely conducted since the STS's External Tank (ET) would reenter over the Pacific, and the predicted breakup would be at a high enough altitude that its debris dispersion pattern would be excessive. At the direction of the OSAF, the STS program manager at JSC along with several key managers and selected astronauts were briefed on the VAST reentry experiment results. NASA management agreed to the Air Force mission profile and, subsequently, conducted tests to eventually verify the ET reentry breakup characteristics. The tank rupture was eventually found to be at a low enough altitude to safely justify the Air Force mission profile.

3. VAST and VASP Experiments

The satellite reentry experiments conducted during the early 1970s involved two different types of satellite vehicles. The first four tests referred to as VAST (Vehicle Atmospheric Survivability Tests) utilized one specific type of satellite vehicle. A second and larger type of satellite vehicle was subsequently used in two tests referred to as VASP (Vehicle Atmospheric Survivability Project). Except for the last two VAST reentries, extensive tracking assets were employed and are summarized in Table 1.

Table 1 summarizes the principal assets used in VAST and VASP. One of two identical tracking ships, ARIS (Advanced Range Instrumentation Ships), was in service while the second was being serviced. The ship could collect telemetry, radar, and optical data. The optical data required clear skies. Optical data was fortuitously available in VAST2 and VASP 1. The IFLOT (Intermediate Focal Length Optical Tracker) acquired images with resolution of 1 ft near the point of closest approach.

The TRAP (Thermal Radiation Airborne Program) carried infrared equipment and visual range optics that tracked reentry and satellite breakup. A PRESS aircraft, similar to TRAP, was operated by the Navy. A large land-based radar at Shemya, Alaska was used when the reentry trajectory path allowed (VAST 1 and VASP 1).

The support summary for the tests is shown in Table 2. Limited support was provided for VAST 3 and 4 since these were payload element retrieval missions. Therefore, on VAST 3 and 4, no tracking of the breakup process was made. The breakup histories of VAST were so consistent that only two

Table 1. Principal Resources

ARIS TRACKING SHIP
Radar: -L Band -C Band -UHF
Optics: - Boresight Cameras -IFLOT
Telemetry: - 30-ft Dish (225 → 2300 MHz)
TRAP AIRCRAFT - OPTICAL TRACKING
TRAP 1
TRAP 7
ARIA TELEMETRY AIRCRAFT
LAND BASED RADARS
Shemya, Alaska
Clear, Alaska
MISCELLANEOUS SUPPORT
Sonobuoys
Cubmarine Underwater Recovery
USN Watertown Surface Recovery

Table 2. Support Summary

VAST/ VASP	Vehicle	Date	Payload Impact	ARIS	TRAP	ARIA	Land-Based Radar	Other
VAST 1	OM 30	9 Feb 71	BOA*	1	2	2	Shemya	USN Watertown
VAST 2	OM 31	13 May 71	BOA*	1	1	2	--	PRESS Aircraft
VAST 3	OM 32	3 Sept 71	Alaska	--	--	--	Clear	--
VAST 4	OM 34	11 April 72	Eniwetok	--	--	--	--	Sonobuoys
VASP 1	SV 5	19 May 73	BOA*	1	--	2	Shemya	--
VASP 2	SV 6	12 Oct 73	Eniwetok	1	1	3	--	Sonobuoys & Cubmarine

*Broad Ocean Area

VASP tests were planned for the larger vehicle even though it was significantly different structurally. The first VASP test confirmed the breakup characteristics, which were predicted from VAST results. VAST 1 and VAST 2 were targeted for reentry in the Western Pacific because of range safety and observation considerations. It is noted that the debris footprint for VAST ranged up to 1,000 nmi. It was the intent of VAST 1, 2, and 4 to stay away from populated land masses. VAST 3 was a payload sensor recovery mission targeted into a remote region of Alaska. VAST 4 was intended to be a payload element recovery mission, and that portion of the 1000-nmi-long footprint was targeted for Eniwetok Lagoon. VASP 1 was targeted into the Western Pacific to utilize the large radar at Shemya, Alaska. The second and final VASP was targeted for payload element recovery in Eniwetok Lagoon. The support for the second VASP had significant tracking to confirm that breakup was consistent with VASP 1, as well as the VAST reentries.

As can be noted in Table 2, both VAST 1 and 2 had the support of two optical tracking aircraft. By 1973, only one optical tracking aircraft was available for the two VASP reentries. The data obtained from that single TRAP on VASP 2, however, was remarkable and extremely informative.

3.1 The Vehicle Atmospheric Survivability Project (VASP)

The satellite vehicle used in the VASP tests was larger and of relatively simple monocoque structure (not a dual vehicle as was VAST). The vehicle did have a boat tail, which resulted in a trim angle of attack of 19° (verified by onboard telemetry). Until initial breakup (loss of boat tail), the vehicle was generating lift. While the lift corrupted the trajectory, the vehicle reached the melting temperature at conditions in accordance with the VAST breakups. Further corroboration of the VAST results was obtained through onboard temperature data collected prior to breakup, which indicated heating an order of magnitude less than obtained by traditional heating analysis.

The VASP 1 breakup was consistent with VAST breakup conditions. The reentry breakup allowed the estimation of the trajectories of the payload elements for which recovery was desired. VASP 2 was targeted such that the desired components would nominally impact in or near Eniwetok Lagoon. The tracking resources of VASP 2 verified that its breakup was similar to VASP 1 and all of the VAST reentries. For this reason, the VASP results were only initially used to confirm similarity to the VAST results.

The payload elements of the VASP vehicles were smaller than those of the VAST vehicles. For this reason, more emphasis was placed on the debris and their characteristics. To accomplish this, VASP 2 was deboosted such that it reentered at night to enhance the optical and spectral data obtained. It is noted that differences in the pre-deboost orbit and available deboost propellant prohibited a night reentry on the VAST tests. It was therefore possible, with VASP 2, to correlate the materials and, in some cases, the component from which the debris evolved.

4. Vehicle Description

Figure 1 presents an inboard profile of a VASP vehicle as configured prior to reentry. The vehicle is a monocoque structure with a magnesium skin. The vehicle approached reentry (under attitude control) with the aft end (orbit adjust engine) facing in the direction of the velocity vector. The total weight of the vehicle at reentry was approximately 11,750 lb.

The vehicle's forward end contained a secondary sensor. It was connected to the aft portion of the vehicle with a beam section open on the bottom and closed on top with magnesium skin. The internal structure was aluminum and magnesium stringers and frames.

The beam section was structurally integrated with the primary sensor compartment. It was structurally similar to the beam section open on the bottom but enclosed with non-structural fiberglass. Two sensors were contained in this compartment supported by an aluminum frame (387 lb). The sensors were complex electro mechanical devices composed of aluminum, Invar, steel, beryllium, and glass.

The sensor support compartment aft of the sensor compartment was a totally enclosed magnesium monocoque structure. This compartment contained a 960-lb electro-mechanical device consisting of two 105-lb motors.

The aft compartment contained the vehicle support equipment. Its contents included batteries, electronics, orbit adjust propellant tank, backup stabilization system propellant tanks, and a payload pres-

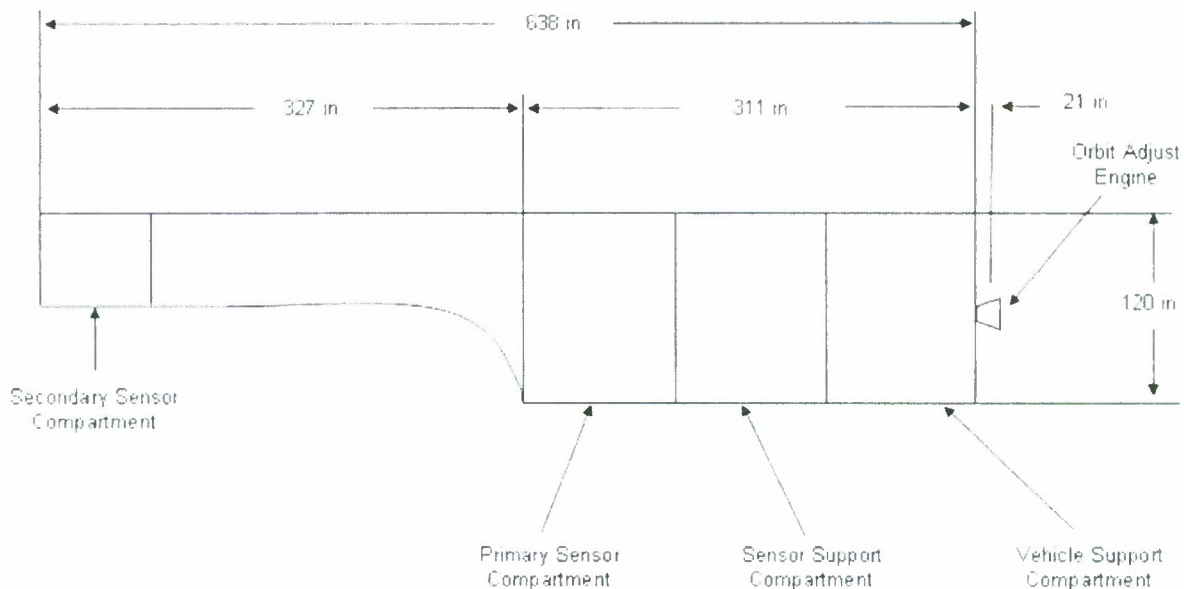


Figure 1. In-board profile VASP vehicle.

surization tank. The vehicle's solar arrays folded out from the aft bulkhead of the vehicle and exited out perpendicular to the vehicle's longitudinal axis.

Quantities, weights, dimensions, materials, and estimated ballistic coefficient are provided in Table 3.

Table 3. Estimated Aerodynamic Characteristics of Various Subsystems

Item	Quantity	Weight (lb)	Approximate Size	Basic Materials	Ballistic Coefficient* (lb / ft ²)
RCS Propellant Tank	4	17	22" D x 0.02" t	Titanium	7
Attitude Control Pressurization Tank	2	58	22" D x 0.2" t	Titanium	24
Orbit Adjust Propellant Tank	1	289	62" D x 0.05" t	Aluminum	15
Payload Pressurization Tank	2	33	18" D	Steel	20
Batteries	4	110	19" x 8" x 9"	<div style="display: flex; align-items: center;"> <div style="font-size: 3em; margin-right: 5px;">{</div> <div style="text-align: center;"> Aluminum Nickel Cadmium Silver Zinc </div> </div>	177
Cells/Battery	22				19
Secondary Sensor	1	225	15" D x 24"	Beryllium	95
Main Sensor	2	930	-	<div style="display: flex; align-items: center;"> <div style="font-size: 3em; margin-right: 5px;">{</div> <div style="text-align: center;"> Aluminum Invar Beryllium Glass </div> </div>	35
Component #1	2	93	Omitted	Omitted	45
Component #2	2	80	Omitted	Omitted	33
Component #3	2	38	Omitted	Omitted	22
Support Equipment Assembly	1	754	90" D x 48"	Aluminum	25

*Hypersonic values below 42 nmi altitude

5. VASP Breakup Sequence

The vehicles employed in VASP were deboosted from Low Earth Orbit with the aft end forward to facilitate deboost. The small orbit adjust engine on the vehicle's aft end provided the deboost velocity increment. The deboost maneuver was conducted under geocentric control with the vehicle's longitudinal (thrust) axis aligned parallel to the Earth's surface and in the plane of the velocity vector. This attitude was maintained thereafter by small reaction control jets.

Onboard telemetry indicated that aerodynamic torques overpowered the RCS jets slightly above 50 nmi (see Tables 4 and 5). The vehicle had a boat tail that provided an aerodynamic angle of attack trim point of 19° in an aft-end-first attitude.

The flexible solar arrays, which did not produce a significant aero torque, folded back against the vehicle under aerodynamic pressure and were still attached to the vehicle at loss of telemetry at about 50.0 nmi altitude (via telemetry Table 4). The FPS 80 radar at Shemya, Alaska observed possible loss of the panels at 45.2 nmi.

The vehicle trimmed out with its angle of attack oscillating about the aerodynamic trim point at 19° (17° VASP 2) with the vehicle doing a slow roll about the velocity vector. The roll rate was caused by the asymmetrical folding of the solar arrays. This caused the aft end to "see" the velocity vector at

Table 4. Significant Events Test 9265 (SV-5). Conducted 19 May 1973

System Time (s)	Event/Comment	Altitude (nmi)
3956	Begin TM Coverage	69.3
4157	Loss of Geocentric Stabilization	52.9
4180	Max Negative Pitch Rate @ Aero Trim Point of 19°	50.8
4182	Begin FPS 80 Radar Coverage	50.6
4185	Max Angle of Attack During First Oscillation = 30°	50.3
4192	Loss of Telemetry / Solar Panels Still Attached	49.7
4229	Begin FPS-0 Metric Data	46.3
4234	ARIS Horizon Break	45.8
4240	FTD Observed Initial Breakoff of Seven Low β Objects	45.2
4246	First ARIS Video Recording	44.6
4261	End FPS-80 Metric Data	43.2
4262	Begin ARIS Metric Data	43.1
4271	Major Vehicle Breakup	42.3
4368	Begin ARIS IFLOT Optical Coverage	29.5
4381	End ARIS IFLOT Optical Coverage	28.6
4382	Lowest Real Time L-Band Altitude Coverage	28.7
4387	End Real Time L-Band Coverage	31.1

Table 5. Significant Events Test 6337 (SV-6). Conducted 12 October 1973

System Time (s)	Event / Comment	Altitude (nmi)
<46527	Geocentric Control Verified by TM	>54.8
46527	Loss of Geocentric Control Authority	54.8
46534	Loss of Geocentric Stabilization	54.3
46535	First ARIS L-Band Video Recording Data	54.2
46550	Begin ARIS Metric Data	52.6
46554	Max Negative Pitch Rate @ Aero Trim Point of 17°	51.8
46557	Solar Panels Fold Back Against Vehicle	51.6
46559	Maximum Pitch Attitude = 22.5°	51.3
46567	Loss of Telemetry	50.4
46580 → 46600	Initial Fragmentation	46.2 → 47.0
46632	Begin Trap Data	43.4
46645	Major Vehicle Breakup	42.0
46655	Begin Trap Spectrographic Data	40.8
46660	Begin Trap DBM-5 Cine Coverage (Metric Data)	40.3
46685	End Real Time Metric Data	37.3
46695	End Trap Spectrographic	36.0
46728	End Trap DBM-5 Cine Coverage (Metric Data)	31.2
46744	End Trap Data	28.5
46920 →	Eniwetok Lagoon Impact Recorded by Sonobuoys	0

an average angle of attack around 19° (17° VASP 2). The vehicle center of mass was such that the boat tail trailed. This attitude behavior remained until the vehicle broke up, which produced aerodynamic lift forces normal to the velocity vector. After the initial major breakup of the external mono-coque structure, the internal components were on individual trajectories. The trajectories were for the most part on ballistic no-lift paths. A few objects were observed to exhibit lift via falling leaf motion and generate crosstrack displacement. The majority of the objects had been shielded from aerodynamic heating prior to breakup. Low-ballistic-coefficient objects would decelerate rapidly and likely survive by avoiding appreciable heating.

Major breakup and the loss of the boat tail occurred at an altitude of 42 nmi. Prior to breakup, the vehicle was oscillating at a relatively high angle of attack. The lifting forces had caused the velocity vector to be nearly horizontal (occasionally climbing). This caused a slow rate of change in aerodynamic heating rates. This allowed the external surfaces to attain a radiation equilibrium condition where the aerodynamic heat input was matched by the heat lost by radiation.

The heat input for a vehicle broadside to the airstream is given as follows from Table 4 of Reference 1.

$$\dot{Q}_{\text{STAG}} = 34.02 \left(\frac{\rho}{\rho_{\text{SL}}} \right)^{0.5} \left(\frac{V}{10000} \right)^3 \text{ BTU/ft}^2\text{s} \quad (1)$$

$$\frac{\rho}{\rho_{SL}} = \text{Ratio of atmospheric density at altitude to that at sea level}$$

$$V = \text{Relative velocity vector (ft/s)}$$

(Note: See Ref. 1 heating rate independent from radius effects)

The velocity at 42 nmi was 25,250 ft/s which results in a stagnation heating rate 2.65 BTU/ft² s.

The heat lost by radiation is

$$\dot{Q}_{RAD} = \epsilon \sigma T^4 \quad (2)$$

Where:

$$\dot{Q} = \text{Radiation heat loss (BTU/ft}^2\text{/s)}$$

$$T = \text{Temperature (Rankine)}$$

$$\epsilon = \text{Emissivity}$$

$$\sigma = \text{Stephen-Boltzmann Constant (4.7583 x 10}^{-13} \text{ BTU/ft}^2\text{/s)}$$

Vehicle breakup is governed by the external structure approaching the melting temperature where structural integrity is lost. The strength of a metal that is rapidly heated (such as during atmospheric reentry) does not appreciably decrease until near melting. The aerodynamic force at this point was relatively low, causing a deceleration of about 0.7 g's. The melting temperature of magnesium is 1660°R, and it's emissivity between 0.67 and 0.87 (Ref. 2). This results in a radiation stagnation heating rate from (Eq. 2).

$$\dot{Q}_{RAD} = 2.42 \text{ BTU/ft}^2\text{/s for } \epsilon = 0.67 \text{ and } T = 1660^\circ\text{R}$$

and

$$\dot{Q}_{RAD} = 3.14 \text{ BTU/ft}^2\text{/s for } \epsilon = 0.87 \text{ and } T = 1660^\circ\text{R}$$

The radiation equilibrium heating rates bracket the predicted stagnation heating rate of 2.65 BTU/ft²/s calculated previously. An emissivity of 0.73 would match the predicted heating rate; or a temperature of 1605°R at an emissivity of 0.87 would produce radiation heat output of 2.65 BTU/FT²/s.

The radar data indicated a massive breakup with the resulting objects having radar cross sections no larger than those of internal components. The breakups of VASP 1 and VASP 2 were very similar with a cluster of objects grouped closely together with low-ballistic-coefficient objects trailing at ever greater distances.

The objective of VASP was to track lead objects contained in the primary sensor compartment. Detailed analysis of radar signatures was limited to objects thought to be sensor components. From specular analysis of radar returns (ARIS) and spectrographic analysis (TRAP), some sensor items were isolated.

Fortuitously, tracking had been concentrated on one of these objects considered to be one of the main sensors. It was cylindrical with a diameter of 2.9 ft and length of 8.9 ft. The object was a complex electromechanical device. The two ends of the cylinder were connected by Invar rods and completely enclosed with a cylindrical aluminum tank to form a pressure vessel. The two ends consisted of a beryllium housing with steel and electric motor components.

After initial satellite breakup at an altitude of 42 nmi, the cylinder continued with a high tumble rate of 10 cycles per second (cps). It was observed to shed low-ballistic-coefficient material. Likely, this was the aluminum outer casing. At an altitude of 31.5 nmi, experiencing 6.25 g's, it separated into two major pieces. The breakup was likely a result of the axial deceleration and high rotation rate. Tracking continued on the lead fragment for another 29 s, down to an altitude of 28.6 nmi, where the aerodynamic heating was about 46% of its peak value at 36 nmi. The two components were composed of Invar, beryllium, steel, and glass, and at this point, would have weighed several hundred pounds each. With heating decreasing and only a slight increase in deceleration (8 g's) ahead, the two ends would survive to impact. Radar indicated little or no fragmentation at termination of track. Radar track had been broken in a failed attempt to acquire more downrange objects of potential interest. The radar attempt failed due to the ship's proximity to the ground track.

Optical coverage by the IFLOT camera system at the time of loss of radar track observed eight major objects. The IFLOT camera collected data for 14 s before losing track at the point of closest approach (PCA). The track period began 15 s after the cylinder was observed to breakup. The IFLOT system had a field of view of 2.6° by 2.6° and was looking 10° uprange of the radar, and therefore could not have tracked the remnants of the cylinder. The ballistic coefficients of the eight objects ranged from 30 to 100 lb/ft². Two of the eight objects observed optically were observed to fragment into two parts. No correlation of these fragments to specific objects was possible.

6. Debris Impact Area

The radar coverage of VASP 1 (SV-5) included debris mapping of the impact area downrange of the ARIS tracking ship. The radar mapping lasted for 17.4 min, starting 2 min after termination of tracking following vehicle breakup. The total number of fragments observed during mapping was estimated to be 200. All objects were in terminal fall and without winds would impact where observed. The mapping is presented in Figure 2. Since the objects are in terminal free fall, no estimate of ballistic coefficient was possible. The radar returns indicate the size of the objects ranged from 2 to 10 in².

Two concentrated areas of debris were observed with a scattering of individual fragments throughout the mapping period. The first concentration of debris (Area 1) was observed between 209° and 210° azimuth and between 6° and 10° elevation angle with respect to ARIS and at a slant range interval of about 150 to 200 km down range. This area of debris was observed eight times in 5.7 min. The second area (Area 2) of concentrated debris was observed at an azimuth of 208° to 224° and an elevation angle of 6° to 8° and at a slant range of approximately 75 to 175 km. This area of debris was scanned eight times in 7.3 min starting 2 min after the scanning of Area 1.

Figure 3 shows the projected impact points of selected objects tracked during the breakup phase. The debris mapping area (terminal fall) shown in Figure 2 is projected on Figure 3. It is evident that the low-ballistic-coefficient items of Figure 2 are in the region of high-ballistic-coefficient projected impacts of Figure 3. This indicates that some high-ballistic-coefficient items continued to fragment shedding light objects.

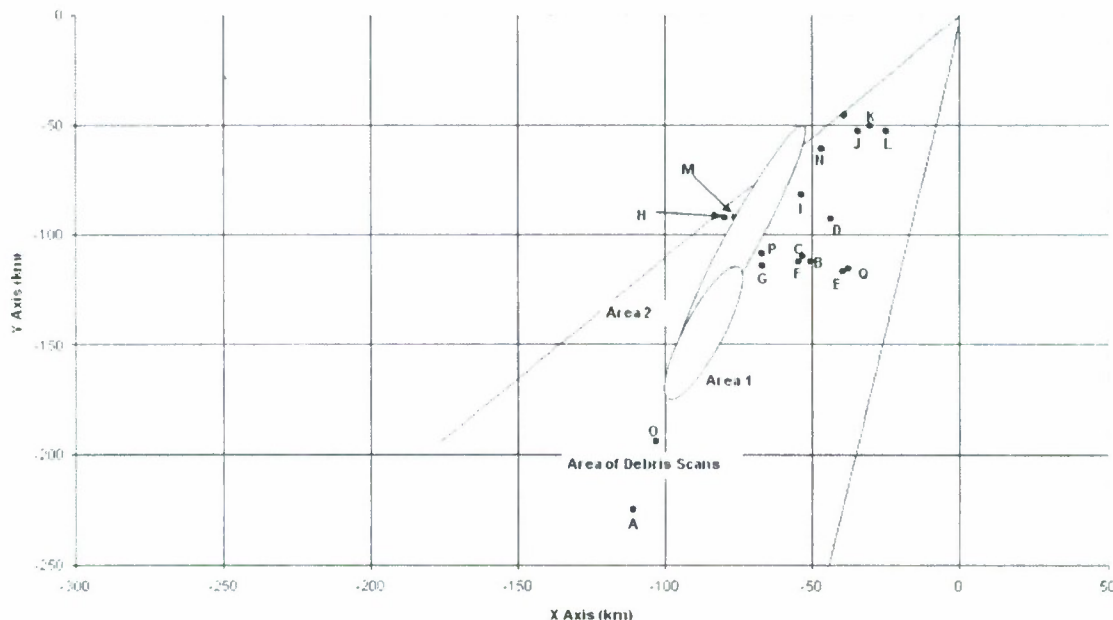


Figure 2. VASP 1 spread of fragments in X-Y plane from debris mapping.

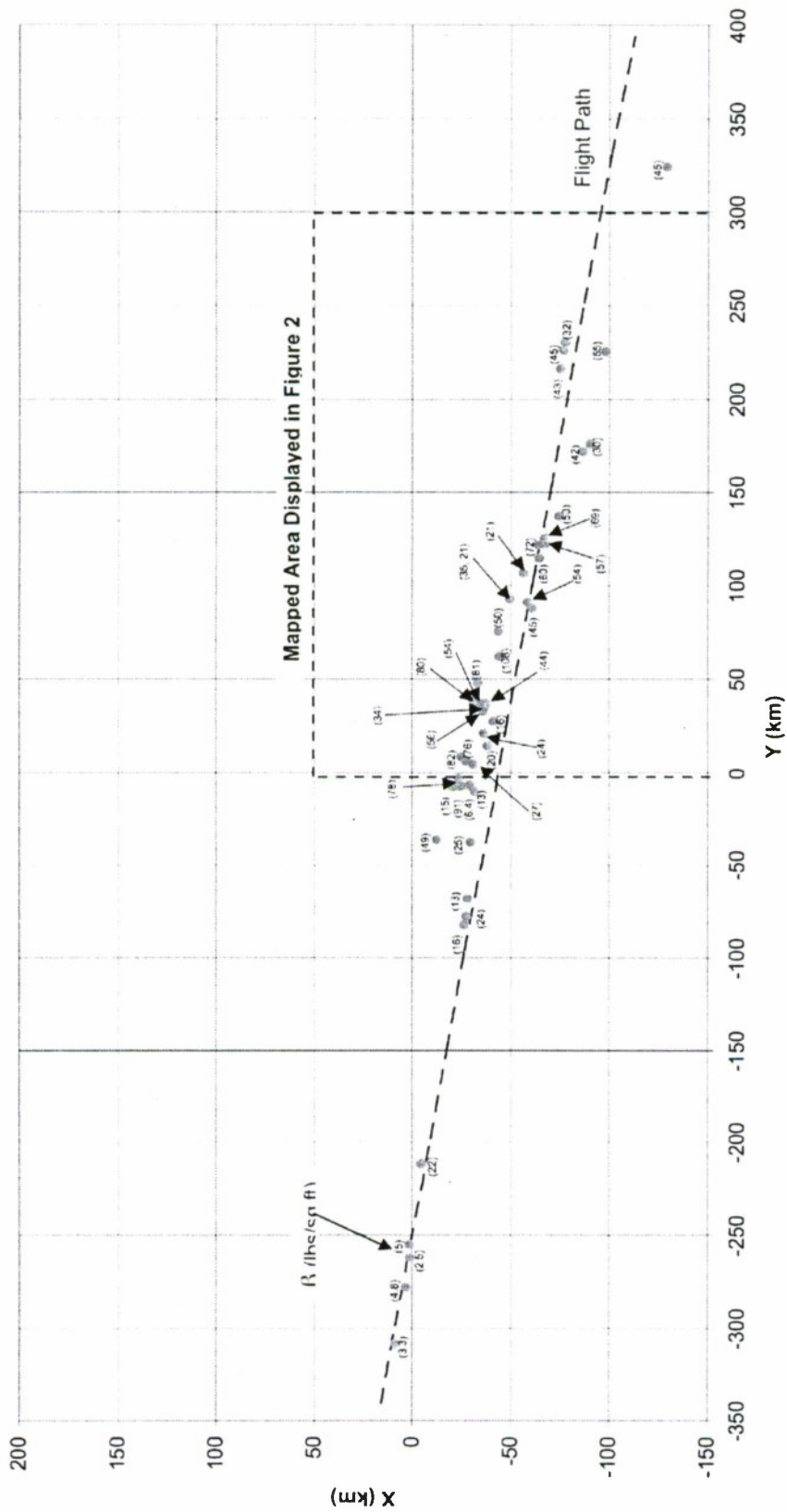


Figure 3. VASP 1 predicted spread of fragments in X-Y plane at impact.

On VASP 2 debris from the Primary Sensor Compartment (Figure 1), including the cylindrical object described in the breakup sequence (Section V), was targeted for Eniwetok Lagoon. Figure 4 shows the projected impact points (observed near terminal fall) in the vicinity of the lagoon.

Lagoon impacts were confirmed by sonobuoys. Time to impact indicated both high-and low-ballistic-coefficient objects impacted. The low-ballistic-coefficient objects were not anticipated but are consistent with the data of Figure 2 for VASP 1. Since the breakup of VASP 1 and 2 were similar, the debris footprint (Figures 2, 3, and 4) should be complementary.

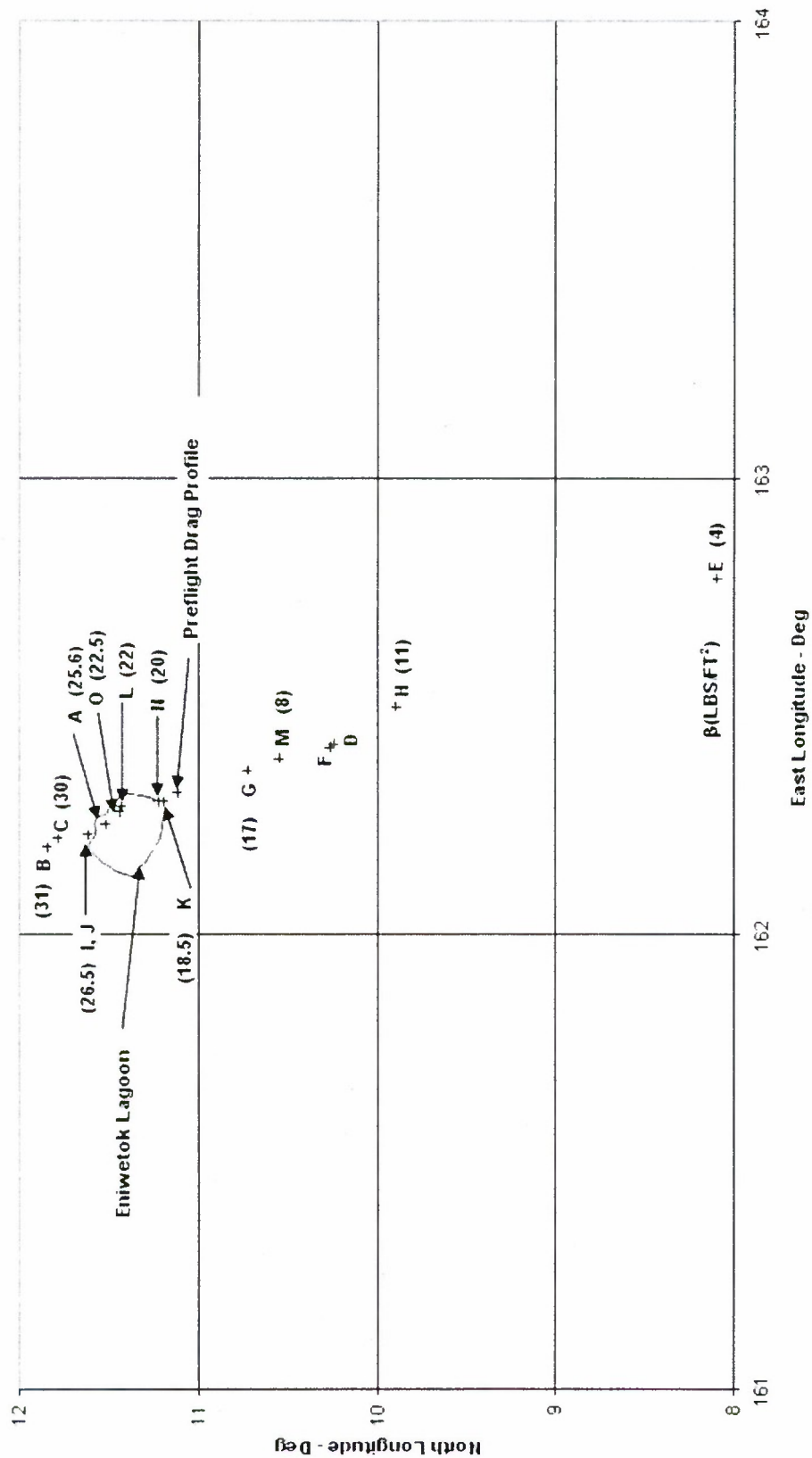


Figure 4. Projected impact points of selected tracked objects of VASP 2 reentry.

7. Hardware Impacting Around Eniwetok

As indicated earlier, the intent of VASP 2 was to target some sensors of the main sensor compartment into Eniwetok Lagoon. Figure 4 depicts the projected impact location of some of these objects. Spectrographic analysis allowed a determination of the object's material make-up. This, coupled with its deceleration behavior, allowed an estimate as to the particular component. Several fragments were observed to be dual objects. Since the main sensor compartment contained two nearly identical sensors, the component identification could be further refined when dual fragments were observed. Table 6 identifies the estimated material make-up and type of component of some objects. The pre-reentry weight and area of each component is provided. No confirmation of the weight or mass impacting the water was available. Sonobuoys did confirm water impacts within the lagoon. Tracked Object A represented a cluster of satellite debris of similar ballistic coefficient fragments. As such, it contained spectrographic evidence of numerous objects representative of the entire satellite, but no

Table 6. Probable Components Projected to Impact In or Near Eniwetok Lagoon

Fragment(s) ID	Impact with Respect to Lagoon (see Fig. 4)	Number of Fragments Observed	Principal Materials Observed (Spectrographic Analysis)	Probable Component	Pre-Reentry Weight – Lb (per Fragment)	Pre-entry Area Ft ² (Per Fragment)	*Ballistic Coefficient (lb/ft ³)
B	Long	1	Beryllium, Aluminum, Magnesium, Glass	Secondary Sensor & Housing	225	1.25	31
C	Long	1	Beryllium, Aluminum, Magnesium, Invar, Glass	Secondary Sensor & Housing	600	3.3	30
I	Long	2	Aluminum, Magnesium, Glass	Main Sensor & Mounting	930	26.0	26.5
J	Long	2	Aluminum, Calcium, Chromium, Iron, Magnesium, Manganese	Motor	103	1.0	26.5
A	Lagoon	Many	Over 20 Materials	Satellite Fragments	?	?	25.6
O	Lagoon	2	Aluminum, Iron, Magnesium, Manganese	Electro Mechanical Assembly	210	3.5	22.5
L	Lagoon	1	Aluminum, Magnesium	Sensor Support Compartment Structure	750	44	22
N	Slightly Short	1	Aluminum, Magnesium	Main Sensor Support	387	15	20
K	Slightly Short	1	Aluminum, Chromium, Magnesium, Manganese, Sodium, Lithium, Titanium	?	?	?	18.5
G	Short	2	Aluminum, Magnesium, Glass	Optical Element	38	3.25	17
M	Short	1	Glass	Optical Element	8	0.25	8
F	Short	1	?	?	?	?	--
D	Short	1	?	?	?	?	--
H	Short	1	Aluminum, Magnesium Glass	?	?	?	11
E	Short	1	Glass	Optical Element	8	0.25	4

*Derived from Tracking Data

specific component could be singled out. This cluster, observed in VASP 1, was used to target the impact point for VASP 2 within the lagoon.

The source of the low-ballistic-coefficient objects impacting the lagoon (evidenced by long descent times) is consistent with Figure 2. Remnants of the massive aluminum primary sensor support frame were also a possible source.

8. Summary and Conclusions

The breakup was consistent with the VAST experiment (Ref. 1) where the outer monocoque structure of the payload section disintegrated suddenly. The disintegration of the monocoque payload observed optically on VAST 2 was total and simultaneous on both the windward and lee sides. This was evidenced on VASP 1 where the disintegration of the monocoque structure was sudden, leaving only individual components and substructures to continue on their trajectories. The initial breakup was consistent with the heating equations derived in Ref. 1 from the VAST experiments. The heating rates that are estimated from Ref. 1 are an order of magnitude less than traditional estimates but are similar to results published in Refs. 3-6.

The impact footprint indicated in Figures 2 and 3 is very prolific but is only a fraction of the objects observed due to limiting the analysis to potential sensor elements. The large survival rate of fragments is due to the less severe heating rate as predicted in Ref. 1 and the presence of electromechanical devices composed of materials with high melting temperatures.

A surprising result of the tests was the presence of very low ballistic coefficient objects in the downrange portion of the impact footprint. This was particularly surprising since radar had indicated a cessation of objects shedding low-ballistic-coefficient fragments well past peak heating. The number and distribution of the fragments is exemplified in Figure 2. These fragments had to evolve from high-ballistic-coefficient objects to achieve their downrange positions. The nature of this evolution is unclear but does suggest a resumption of melting at lower altitudes. The presence of light fragments was consistent throughout the mapped area.

Reference 1 indicated that above an altitude of 30 nmi, reentry heating is reduced by an order of magnitude from traditional heating estimates. The heating equations derived in Ref. 1 are summarized in Table 7. The heating effect on small objects is based upon a specific structure and may not be appropriate for some radii or structural configurations. In any case, the effect on larger radii (one foot or more) seems well founded. Based upon recovered hardware (not from VASP 2), in some cases, Ref. 1 heating estimates are valid below 30 nmi. In cases where the equations of Ref. 1 were no longer applicable (below 30 nmi), traditional heating analysis is appropriate with an order of magnitude increase in heating, which would likely induce melting. The radar mapping results, therefore, probably confirm the cessation, in some cases, of the heating rates derived in Ref. 1 below an altitude of 30 nmi. The low-ballistic-coefficient objects (probably less than 0.25 lb/ft^2) existing in the downrange portion of the debris footprint are likely products of melting followed by cooling and reformation of chaff-like objects.

The data of this report shows that debris will impact over a wide range of times across the debris footprint, with post-breakup debris near the heel (defined by low ballistic coefficient impacts) impacting sooner if there are secondary breakups, and higher ballistic coefficient debris reaching the ground sooner. Additionally, this data has shown that it can take a significant amount of time for debris to impact near the toe of the debris footprint if there are secondary breakups of high-ballistic-coefficient objects resulting in lower ballistic coefficient debris that requires ten's of minutes to impact the Earth's surface.

Table 7. VAST Empirical Heating Rates

-
- Stagnation Point Heating, \dot{Q}_{STAG}

$$\dot{Q}_{\text{STAG}} = 34.02 \left(\frac{\rho}{\rho_{\text{SL}}} \right)^{0.5} \left(\frac{V}{10000} \right)^3 \text{ BTU/ft}^2\text{s}$$

$\frac{\rho}{\rho_{\text{SL}}}$ = Ratio of atmospheric density at altitude to that at sea level

V = Relative velocity vector (ft/s)

- Side Heating, \dot{Q}_{SIDE}

$$\dot{Q}_{\text{SIDE}} = 0.89 \dot{Q}_{\text{STAG}}$$

- Effect of Radius

- No increase for most radii
 - For radii < 2 in., increase heating by 40%
-

References

1. Stern, R. G., "Aerothermal Heating for Satellite Reentry Conditions," Aerospace Report No. TR-2004(8506)-2, September 2004.
2. *Satellite Thermal Control Handbook*, Spacecraft Thermal Department, The Aerospace Corporation, 1994.
3. Lyne, J. E., Tauber, M. E., and Fought, R. M., "An Analytical Model of the Atmospheric Entry of Large Meteors and Its Application to the Tunguska Event," *The Journal of Geophysical Research* **101**(E10), pp. 23207-23212, 1996.
4. Lyne, J. E. and Tauber, M. E., "The Tunguska Event," *Nature* **375**(6533), pp.638-639, 1995.
5. Lyne, J. E., Tauber, M. E., and Fought, R. M., "A Computer Model of the Atmospheric Trajectory of the Tunguska Object," invited presentation at the International Tunguska '96 Workshop, Bologna, Italy, July 15-17, 1996.
6. Lyne, J. E. and Tauber, M. E., "An Analysis of the Tunguska Event," AIAA Paper 95-3477, presented at the 1995 AIAA Atmospheric Flight Mechanics Meeting, Baltimore, MD, August, 1995.
7. Stern, R. G., "Aerothermal Implications of VAST Breakup Sequence," Aerospace Report No. TOR-2000(8504)-10, June 2000.
8. Stern, R. G., "Atmospheric Reentry History and Survival of a Large Solar Array," Aerospace Report No. TOR-2001(8456)-1165, August 2001.
9. Stern, R. G., "Analysis of Mir Reentry Breakup," Aerospace Report No. TR-2003(8506)-1, February 2003.